SCIENCE CHINA
Information Sciences

July 2020, Vol. 63 170201:1–170201:10
https://doi.org/10.1007/s11432-019-2748-x

• RESEARCH PAPER •
Special Focus on Bio-Robotic Systems: Modeling, Design, Control and Perception

Bio-inspired robotic impedance adaptation for human-robot collaborative tasks

Chao ZENG[1], Chenguang YANG[1*] & Zhaopeng CHEN[2]

[1]*School of Automation Science and Engineering, South China University of Technology, Guangzhou* 510641*, China;*
[2]*TAMS Group, Informatics, University of Hamburg, Hamburg* D22527*, Germany*

Received 18 June 2019/Revised 18 July 2019/Accepted 29 November 2019/Published online 26 May 2020

Abstract To improve the robotic flexibility and dexterity in a human-robot collaboration task, it is important to adapt the robot impedance in a real-time manner to its partner's behavior. However, it is often quite challenging to achieve this goal and has not been well addressed yet. In this paper, we propose a bio-inspired approach as a possible solution, which enables the online adaptation of robotic impedance in the unknown and dynamic environment. Specifically, the bio-inspired mechanism is derived from the human motor learning, and it can automatically adapt the robotic impedance and feedforward torque along the motion trajectory. It can enable the learning of compliant robotic behaviors to meet the dynamic requirements of the interactions. In order to validate the proposed approach, an experiment containing an anti-disturbance test and a human-robot collaborative sawing task has been conducted.

Keywords impedance learning, biomimetic control, human-robot collaboration

Citation Zeng C, Yang C G, Chen Z P. Bio-inspired robotic impedance adaptation for human-robot collaborative tasks. Sci China Inf Sci, 2020, 63(7): 170201, https://doi.org/10.1007/s11432-019-2748-x

1 Introduction

In the society of robotics, human-robot collaboration systems have already been known to play an important role in a number of task scenarios including collaborative sawing, carrying, and assembling [1–3]. Human-robot collaboration systems come with many benefits. The most important one is that it brings together the advantages and strengths of both the human side (e.g., flexibility, cognition, understanding the circumstances, decision making) and the robotic side (e.g., superior efficiency, high accuracy) [4–6]. However, the increasing critical requirements of today's high-mix, low-volume, and large-variant industrial manufacturing lines cannot be satisfied by the traditional fully robotic manufacturing systems or by fully human handwork; thus, human-robot collaboration is a promising solution to this dilemma with the integration of the human flexibility and adaptability to bio-robotic manufacturing systems [7, 8].

In this domain, one of the main problems is how to make the robot collaborate with its human partner in a compliant manner. This is because, on one hand, the compliant collaboration is quite important to ensure the safety of both the human and the robot when doing a task in a physical dynamic environment [9]. On the other hand, learning to work compliantly with the human partner for a particular manipulation task is indeed a demand for the robot. As a matter of fact, it is usually expected for the robot to be capable of compliant manipulation in a physical interaction [10], regardless of whether or not they collaborate with humans. However, in a human-robot collaboration scenario, this kind of compliance demand becomes a crucial problem because the robot and its human partner have to adapt to each other during the task execution, to satisfy the constraints in terms of motion and force domains [11, 12].

* Corresponding author (email: cyang@ieee.org)

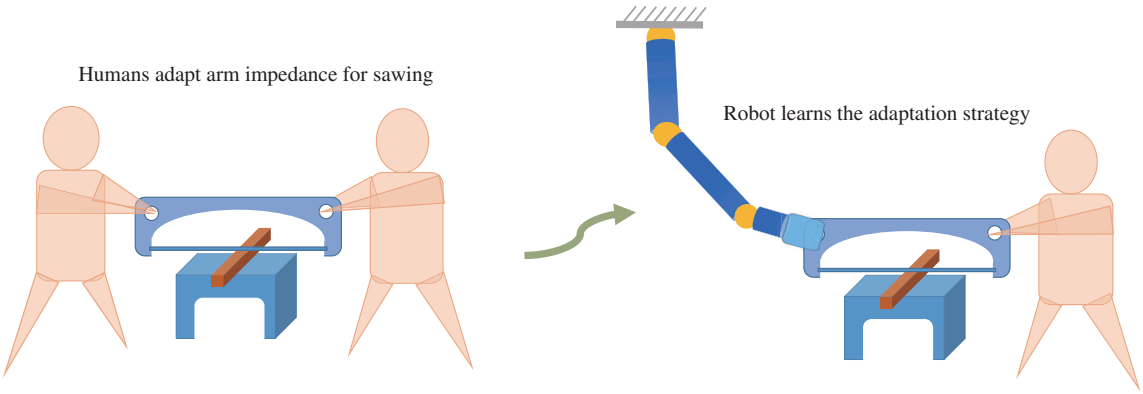

Figure 1 (Color online) The overview of the proposed approach. In a human-human collaboration scenario one human partner will adapt his arm impedance/force to another partner in a real time manner, thus enabling flexible execution of the task. Our approach can allow the robot to learn the human impedance online adaptation strategy and to implement it in a human-robot collaboration system.

A number of approaches have been introduced in the field of robotic control to address the above problem [13–17]. Among these approaches, impedance adaptation has presented its effectiveness in a large number of task scenarios (see, e.g., [18–20]), and it has been widely discussed in the recent decades. The variable impedance controller that represents a relationship between the position and force with variable gains can enable the robot to behave in a compliant manner, i.e., larger gains correspond to higher impedance and vice versa. The only problem is how to obtain the desired impedance profiles.

To date, there have been several approaches proposed to achieve this goal. Typically, bio-signals (i.e., electromyography (EMG)) have been widely used to account for the variable impedance in a human-robot interaction system [21–23]. The stiffness of the human arm is first estimated based on the EMG signals and then transferred to the robot through a proper stiffness mapping mechanism. This approach can enable the transfer of the impedance features of the human partner to the robot. However, the stiffness estimation follows a complicated and time-consuming procedure, which makes it difficult to use in a human-robot collaboration task. Reinforcement learning techniques have also been introduced to learn variable stiffness profiles [24–26]. Stiffness profiles are initialized with constant values and refined through a trial-and-error method and adapted based on the cost functions. However, it may be difficult to define a proper cost function for this, which may result in requiring a large number of trials. More importantly, it is quite different to apply this approach in a collaborative task because of the large uncertainties potentially driven by the human partner. Another approach is to create a relationship between the stiffness and interaction force collected from a force/torque sensor that is mounted onto the robotic end-effector [27–30]. Often, this relationship can be encoded through machine learning techniques such as the Gaussian mixture model and hidden Markov model [27]. An offline estimation procedure is also required. The stiffness is learned based on the force signals, which suffer from the force noises.

In this study, we propose an online learning approach to address this problem. The proposed bio-inspired approach is based on the biomimetic controller which is derived from the human motor learning precipices [29, 30]. The impedance profiles are adapted along the motion trajectories through the interaction between the human and the robot in an online manner. We verify our approach in a usual collaborative scenario, i.e., a sawing task. The main idea of our approach is presented in Figure 1.

2 Methodology

In Section 2, we will show the impedance adaptation approach, based on the human-like biomimetic control strategy.

2.1 Impedance control model

For the human-robot collaboration task, i.e., sawing task, the configuration of the robotic arm is first "fixed" using an impedance control model. The dynamic model of the robotic arm with N DOFs (degree of freedoms) can often be expressed as [11,30]

$$M(q)\ddot{q} + C(q,\dot{q})\dot{q} + G(q) = \tau_c + \tau_e, \tag{1}$$

where q and $\dot{q}$ are the joint angle and the velocities of the robot arm, respectively. $M(q)$ and $G(q)$ represent the robotic arm's inertia matrix and gravity vector, respectively. $C(q,\dot{q})$ represents the Coriolis and centrifugal forces. τ_c and τ_e are the control torque and the external torque, respectively.

According to the human arm motor learning strategy, the control input τ_c can be defined as a feedforward term plus a feedback term:

$$\tau_c = u + v, \tag{2}$$

where u and v are the feedforward torque and the feedback, i.e., impedance term, respectively. The impedance term is defined as

$$v = Ke + D\dot{e} \tag{3}$$

with

$$\begin{cases} e = q_0 - q, \\ \dot{e} = \dot{q}_0 - \dot{q}, \end{cases} \tag{4}$$

where e and $\dot{e}$ represent auxiliary angle and auxiliary velocity error vector, respectively. q_0 and $\dot{q}_0$ represent the desired angle and velocity of a default posture, respectively. K and D are the joint stiffness matrix and damping matrix, respectively, which are both diagonal as

$$\begin{cases} K = \mathrm{diag}\{k_1, k_2, \ldots, k_N\}, \\ D = \mathrm{diag}\{d_1, d_2, \ldots, d_N\}. \end{cases} \tag{5}$$

The elements of the stiffness matrix will be adapted based on the task situation, which will be detailed in Subsection 2.2. The damping matrix is calculated according to the stiffness as $D_{ii}^t = \eta\sqrt{K_{ii}^t}$ at each time step, with the predefined positive constant coefficient η, and $i = [1, 2, \ldots, N]$.

2.2 Biomimetic adaptive control law

The biomimetic controller developed in [29] is extended and utilized for the learning of the compliant behaviors of a redundant robot manipulator with high-dimension DOFs. The graphic diagram of the biomimetic controller is illustrated in Figure 2.

The following cost function was considered in [29] for the concurrently minimizing of the motion error and the effort:

$$J_{\mathrm{cost}} = \frac{\alpha}{2} v^{\mathrm{T}} v + \sum_{i=1}^{N} \gamma_i u_i, \tag{6}$$

where α and γ are the N dimension parametric vectors. $\alpha_i > 0$ and $\gamma_i > 0$ account for the corresponding ith joint's impedance and feedforward torque, respectively. The first term represents the cost for motion error, and the second term, i.e., the weighted sum of the feedforward, represents the cost for effort.

For the ith joint, the impedance term v_i can be assumed as a linear function which increases in both positive and negative directions. This assumption is inspired by one of the principles of the human motor learning, which can be expressed as

$$v_i = \varepsilon_{i,+} + \zeta\varepsilon_{i,-}, \quad \zeta \in (0,1), \tag{7}$$

where $\varepsilon_{i,+}$ and $\varepsilon_{i,-}$ denote the positive and negative directions, respectively, and they are determined by

$$\begin{cases} \varepsilon_i = \pi(e_i + \delta\dot{e}_i), \\ \varepsilon_{i,+} = \max(\varepsilon_i, 0), \\ \varepsilon_{i,-} = (-\varepsilon)_{i,+}, \end{cases} \tag{8}$$

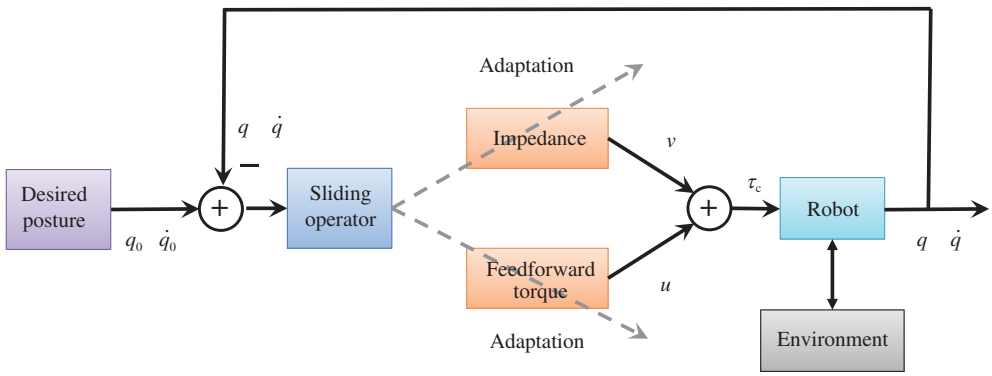

Figure 2 (Color online) The diagram of the biomimetic controller.

where π and δ are positive coefficients, and ε is the sliding error vector.

The learning of (6) can be considered as a gradient descent problem, i.e.,

$$\Delta u^t = u^{t+1} - u^t = -\frac{\partial J_{\text{cost}}}{\partial u}, \tag{9}$$

then yielding the following law:

$$\Delta u^t = \alpha v^t - \gamma. \tag{10}$$

Based on (7) and (8), the adaptation law can be divided into three parts: an antisymmetric part, a symmetric part, and a bias.

$$\Delta u^t = \frac{\alpha}{2}(1-\zeta)\varepsilon^t + \frac{\alpha}{2}(1+\zeta) \mid \varepsilon^t \mid -\gamma \tag{11}$$

with

$$\mid \varepsilon \mid = (\mid \varepsilon_1 \mid, \mid \varepsilon_2 \mid, \ldots, \mid \varepsilon_N \mid). \tag{12}$$

Accordingly, the following update law can be derived from the above cost function:

$$\Delta u_i^t = \alpha \varepsilon_i^t, \tag{13}$$

$$\Delta K_{ii}^t = \beta \mid \varepsilon_i^t \mid -\gamma_i. \tag{14}$$

A relaxation factor term is then set into the feedforward updating law, according to the consideration that the robot joints lack fatigue properties. We consider the following relaxation factor:

$$\Delta u^t = \alpha \varepsilon^t - \frac{1}{\exp(\mid \varepsilon^t \mid)} u^t. \tag{15}$$

Finally, we adapt the bias, i.e., γ, according to the sliding error at each time step rather than using a constant vector.

$$\gamma_i = \frac{a}{1 + b \mid \varepsilon_i \mid}, \tag{16}$$

where a and b are pre-defined positive constant coefficients. By using this equation, at each time step γ_i can regulate the increment impedance of the corresponding joint based on the motion error. Thus, Eq. (14) is modified as

$$\Delta K_{ii}^t = \beta \mid \varepsilon_i^t \mid - \frac{a}{1 + b \mid \varepsilon_i^t \mid}. \tag{17}$$

This learning law may result in the positive values of the joint stiffness matrix, which makes no sense in the real-word implementation. To avoid this problem, the elements of the stiffness matrix are adjusted in a proper range by

$$K_{ii}^t = \begin{cases} K_{ii}^{\max}, & \text{if } K_{ii}^t > K_{ii}^{\max}, \\ K_{ii}^{\min}, & \text{if } K_{ii}^t < K_{ii}^{\min}, \\ K_{ii}^t, & \text{otherwise}, \end{cases} \tag{18}$$

with the pre-set $K_{ii}^{\max}$ and $K_{ii}^{\min}$ in accordance with the robotic platform.

The complete updating process for the learning of the robotic compliant movement is summarized in Algorithm 1. For more details about the biomimetic control law, please refer to [29].

Algorithm 1 The online learning of the robotic compliant movement

Input: The desired robot arm posture (q_0, $\dot{q}_0$);
Output: The computed joint torque command τ_c^t by (2) at each time step;
Initialize the stiffness and damping matrix as $K^0 = \text{diag}\{0, 0, \ldots, 0\}$ and $D^0 = \text{diag}\{0, 0, \ldots, 0\}$;
Initialize the feedforward vector as $u^0 = \text{diag}\{0, 0, \ldots, 0\}$;
Set the constant coefficients π, δ, a, and b;
Set the constant parametric vectors α and β;
Set the stiffness range $K^{\max}$ and $K^{\min}$;
for each time step $t \in [1, T]$ **do**
  Get the current robot joint states q and $\dot{q}$;
  Compute the angle error and the velocity error according to (4);
  Compute the sliding error according to (8);
  Compute the vector γ according to (16);
  Update the feedforward torque $u^{t+1} = u^t + \Delta u$, using (15);
  Update the stiffness matrix $K^{t+1} = K^t + \Delta K$, using (17);
  Adjust the stiffness values in a proper range based on (18);
  Compute the damping matrix D^{t+1};
  Compute the impedance term v^{t+1};
  Compute the joint torque τ_c^{t+1}, using (2);
  Send the joint torque command to the robotic joint motors;
end for

3 Experiment

3.1 Robotic platform

In our experiment, we use a Baxter robot with two arms as our robotic platform; one of the arms is used to perform the tasks. The arm has 7 joints, i.e., two shoulder joints (S0 and S1), two elbow joints (E0 and E1), and three wrist joints (W0, W1, and W2), as shown in Figure 3. An interface for direct joint torque control is provided in the robot itself, which can make the implementation of the proposed approach quite convenient. The robot is controlled in the robot operating system (ROS) with a control rate of 1000 Hz.

3.2 Tasks

In this subsection, there have been two tasks performed, i.e., a test of the anti-disturbance task and a collaborative sawing task.

3.2.1 *Test of anti-disturbance*

The first task is the anti-disturbance test. The goal of this task is to validate the ability against eternal disturbance using the proposed approach. A human would increase his arm strength when external disturbance exerts on this arm, which is significantly important for interactions with the environment. We would like to illustrate if the robot is able to learn this human's strength/impedance adaptability using our approach.

The experimental set-up is shown in Figure 3(a). It shows that the robot's partner applies disturbance on the robot arm by shaking the arm irregularly. The settings of the parameters of this experiment are $\pi = 1.3$, $\delta = 0.01$, $\beta = [1.0, 1.0, 0.4, 3.5, 0.3, 0.3, 0.5]^{\mathrm{T}}$, $\alpha = [8.0, 8.0, 8.0, 8.0, 8.0, 8.0, 8.0]^{\mathrm{T}}$, $a = 0.1$, $b = 10$, $K_{\min} = \text{diag}\{5, 5, \ldots, 5\}$, and $K_{\max} = \text{diag}\{200, 200, \ldots, 200\}$.

The experimental results of the task are shown in Figures 3(b)–(h). They present the joint angle, the measured torque, and the learned stiffness of the seven joints (i.e., S0, S1, E0, E1, W0, W1, and W2), which correspond to the seven subplots. It can be clearly observed that the stiffness could increase immediately to resist the disturbance by the human tutor once the robot arm configuration is in the departure from the desired posture (from about 2 to 16 s), and the stiffness would decrease to the default value to be compliant once the disturbance is removed, which is very similar to the human experience. Aside from that, the stiffness profiles of the first four joints (i.e., S0, S1, E0, and E1) have been adapted more largely than those of the last three joints (i.e., W0, W1, and W2). This can be explained by the

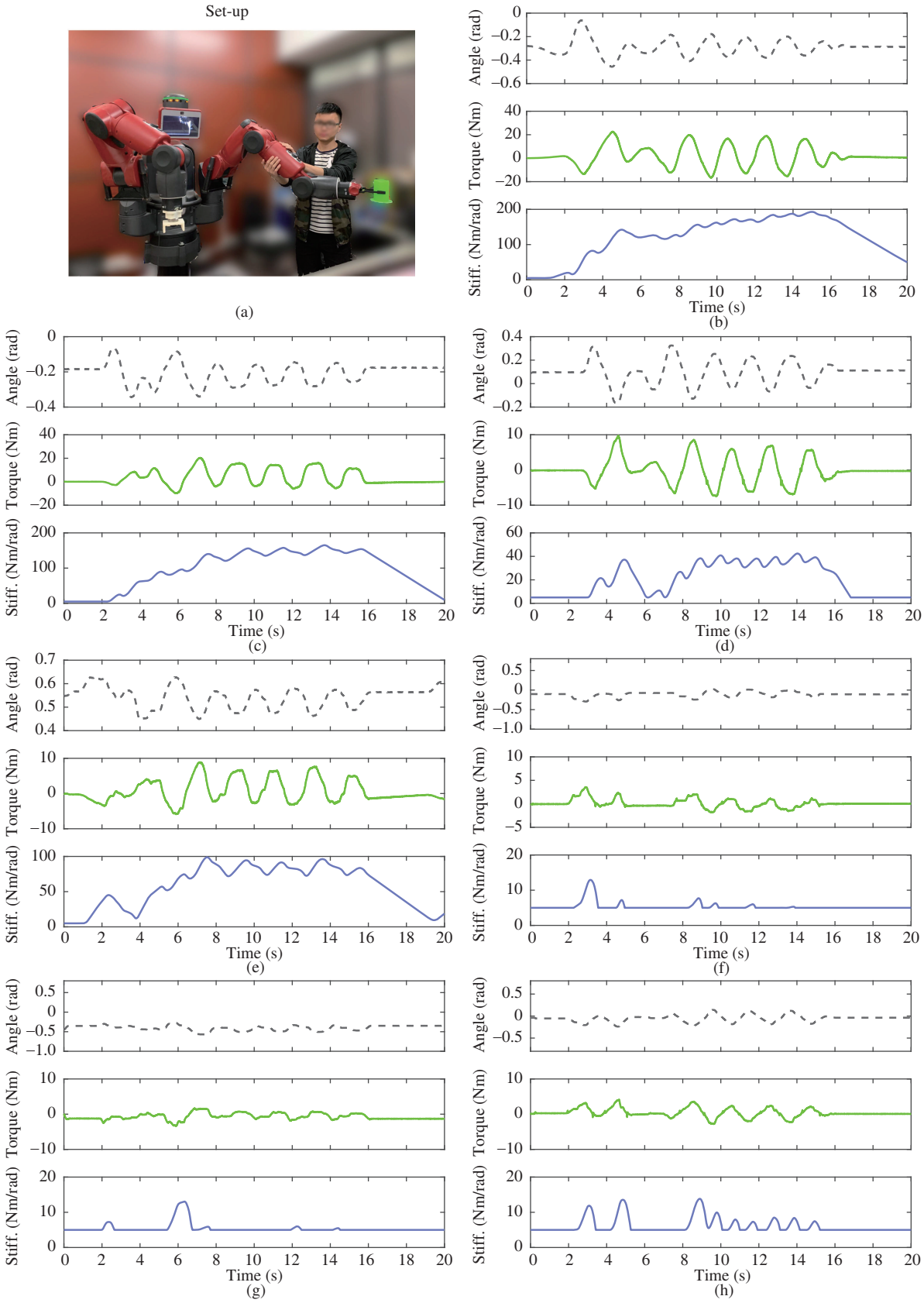

Figure 3 (Color online) The set-up (a) and the results of the disturbance test of (b) joint S0, (c) joint S1, (d) joint E0, (e) joint E1, (f) joint W0, (g) joint W1, and (h) joint W2.

Figure 4 (Color online) The experimental set-up for the sawing task. (a) The human partner actively pulls the saw. The impedance of the robotic arm increases gradually from a small value to some extent. (b) The robot actively pulls the saw back owing to the large impedance. The human partner relaxes his muscle strength in this phase.

fact that the first joints have been affected much more largely by the disturbance than the other three joints.

3.2.2 *Human-robot collaborative sawing*

The second task we perform is a sawing task completed through the collaboration between the human partner and the robot. Human-robot sawing is a typical task scenario where the robot's flexibility and adaptability are required. In a human-human sawing system, one partner must directly adapt his arm strength to the other one in every cycle. Accordingly, they must collaborate well with each other; otherwise, the task cannot be completed efficiently. A good performance of collaboration in "muscle" space with each other is also needed in the human-robot sawing system.

The experimental set-up for this task is shown in Figure 4. It shows how the human partner collaborates with the robot to saw a piece of wood during the execution of this task. One side of the saw is mounted onto the end-effector of one of the robotic arms, and the wood is mounted onto the fixture which is attached on the surface of a table. The settings for the sawing task are given as follows: $\pi = 1.3$, $\delta = 0.008$, $\beta = [5.0, 2.0, 0.6, 0.2, 0.2, 0.24, 0.75]^{\mathrm{T}}$, $\alpha = [5.0, 5.0, 5.0, 5.0, 5.0, 5.0, 5.0]^{\mathrm{T}}$, $a = 0.6$, $b = 12$, $K_{\min} = \mathrm{diag}\{5, 5, \ldots, 5\}$, and $K_{\max} = \mathrm{diag}\{100, 100, \ldots, 100\}$.

The experimental results are presented in Figure 5. Again, it presents the joint angle, the measured joint torque, and the learned stiffness profiles of the seven joints of the robotic arm. First of all, the robot's adaptation behavior is presented as expected: the joints S1, E1, and W1 are mainly involved in this task whose stiffness profiles, therefore, have been adapted, while those of the other three joints remain at the default value because these four joints stay at the desired posture during the sawing process. It can be observed that the stiffness profiles are adapted with the change of the joint angles in every cycle. In the first half cycle, the human partner pulls the saw, and the robot follows the movement of the saw, while the stiffness of the relevant joint increases because of the increasing angle error. When the robot arm impedance becomes large to some extent, the robot arm would behave like a spring and pull the saw back. This process can be seen as the second half cycle, during which the stiffness would decrease to a small value. In this way, the human partner and the robot can collaborate well with each other to complete the sawing task.

3.3 Discussion

In a human-robot interaction or collaboration scenario, the robot is expected to be capable of automatically adapting its impedance/force to deal with the external disturbance from the environment including humans or to meet the requirements of the tasks. The proposed approach has achieved this goal and has enabled the robot with high DOFs to successfully acquire the humanlike adaptability with the help of the biomimetic controller derived from the principles in human motor learning. The experimental

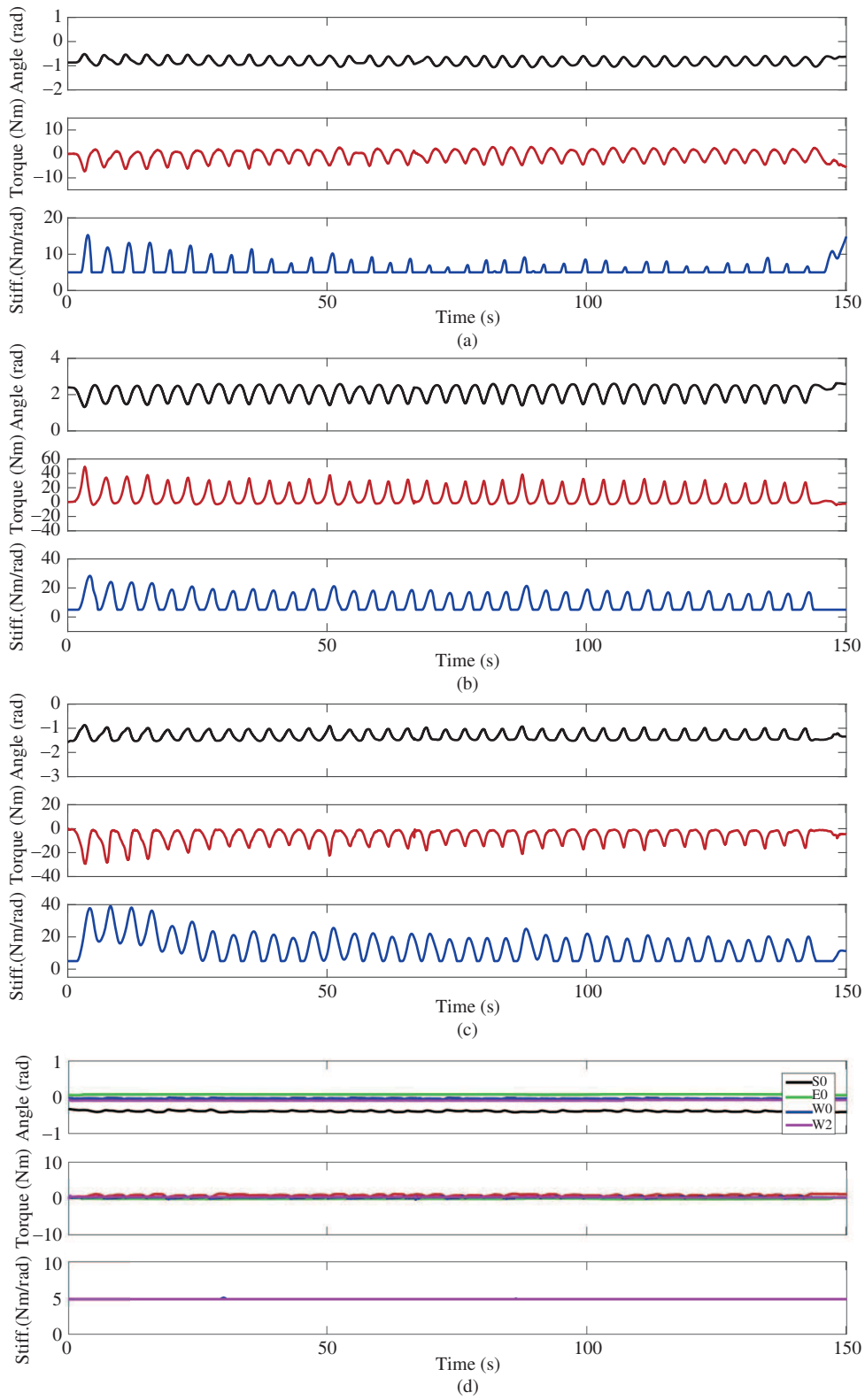

Figure 5 (Color online) The experimental results of the sawing task. (a) Joint S1; (b) joint E1; (c) joint W0; (d) joints S0, E0, W0, and W2.

results show that the robot has demonstrated the compliant behaviors. Additionally, the robot is able to selectively increase/decrease the stiffness/force profiles of the appropriate joints to adapt to the task situations, owing to the proposed stiffness learning mechanism.

Compared with the state-of-the-art approaches in this domain, our approach can present several advantages. First of all, the efficiency of learning of stiffness is one of the main powerful points of our algorithm. The impedance profiles can be learned in a real-time manner along with the movement trajectories. The impedance is adapted according to the motion tracking performance, i.e., keeping the desired posture in our case, and it can enhance this performance as well. A large number of trials would not be required with our approach, while other approaches often require such trials (e.g., reinforcement learning techniques).

Another advantage of the proposed approach is that it can enable simultaneous learning of the impedance profiles and the feedforward torques. However, other approaches only enable the separate learning of one of the two terms. Although the feedforward torque is not particularly emphasized in our usage, it can indeed play a great role in the domain of skill generalization. Therefore, our approach can potentially be applied in both skill learning and skill generalization of robotic compliant movements.

Additionally, we do not need to add a force sensor onto the end-effector of the robotic arm to collect the interaction force data between the robot and its environment for adaptation of the robotic arm impedance, while most of the state-of-the-art approaches need to do so.

4 Conclusion and future work

In this study, we proposed a bio-inspired approach that could enable the robot to learn compliant behaviors from the interactions and collaborations with the human partner. A biomimetic control strategy inspired by the human arm motor control is utilized to adapt feedforward torque and the impedance in the dynamical environment simultaneously. Specifically, the descent impedance profiles can be learned online along with the motion trajectories based on the task requirements, making our approach efficient and superior among most of the state-of-the-art approaches. The human-robot interaction disturbance test and the human-robot collaboration sawing task conducted on the Baxter robotic arm with seven joints have demonstrated the effectiveness of the proposed approach.

There are several potential ways that may be utilized to improve the proposed approach. Future work might be mainly focused on the following two aspects.

(1) We will consider implementing the biomimetic controller in the task space of the robotic arm. The goal is not only to learn the stiffness profiles in translational directions but also to learn the stiffness profiles in rotational directions.

(2) Our approach may be improved and used in a robotic system that has much higher DOFs such as a robotic hand-arm coordination control system. Impedance profiles of both the hand and the arm are learned and adapted simultaneously for flexible and dexterous manipulations.

Acknowledgements This work was supported by National Natural Science Foundation of China (Grant Nos. 61861136009, 61811530281).

References

1 Peternel L, Petrič T, Oztop E, et al. Teaching robots to cooperate with humans in dynamic manipulation tasks based on multi-modal human-in-the-loop approach. Auton Robot, 2014, 36: 123–136
2 Li Y, Tee K P, Yan R, et al. A framework of human-robot coordination based on game theory and policy iteration. IEEE Trans Robot, 2016, 32: 1408–1418
3 Li Y, Tee K P, Yan R, et al. Adaptive optimal control for coordination in physical human-robot interaction. In: Proceedings of the 2015 IEEE/RSJ International Conference on Intelligent Robots and Systems (IROS), 2015. 20–25
4 Li Y, Ge S S. Human-robot collaboration based on motion intention estimation. IEEE/ASME Trans Mechatron, 2014, 19: 1007–1014
5 Wu Y, Wang R, D'Haro L F, et al. Multi-modal robot apprenticeship: imitation learning using linearly decayed DMP+ in a human-robot dialogue system. In: Proceeding of the 2018 IEEE/RSJ International Conference on Intelligent Robots and Systems (IROS), 2018. 1–7
6 Wang R, Wu Y, Chan W L, et al. Dynamic movement primitives plus: for enhanced reproduction quality and efficient trajectory modification using truncated kernels and local biases. In: Proceedings of the 2016 IEEE/RSJ International Conference on Intelligent Robots and Systems (IROS), 2016. 3765–3771

7 Chen F, Sekiyama K, Cannella F, et al. Optimal subtask allocation for human and robot collaboration within hybrid assembly system. IEEE Trans Automat Sci Eng, 2014, 11: 1065–1075
8 Ko W K H, Wu Y, Tee K P, et al. Towards industrial robot learning from demonstration. In: Proceedings of the 3rd International Conference on Human-Agent Interaction, 2015. 235–238
9 He W, Dong Y, Sun C. Adaptive neural impedance control of a robotic manipulator with input saturation. IEEE Trans Syst Man Cybern Syst, 2016, 46: 334–344
10 Denisa M, Gams A, Ude A, et al. Learning compliant movement primitives through demonstration and statistical generalization. IEEE/ASME Trans Mechatron, 2016, 21: 2581–2594
11 Yang C, Ganesh G, Haddadin S, et al. Human-like adaptation of force and impedance in stable and unstable interactions. IEEE Trans Robot, 2011, 27: 918–930
12 Burdet E, Ganesh G, Yang C, et al. Interaction force, impedance and trajectory adaptation: by humans, for robots. In: Experimental Robotics. Berlin: Springer, 2014. 331–345
13 Ficuciello F, Villani L, Siciliano B. Variable impedance control of redundant manipulators for intuitive human-robot physical interaction. IEEE Trans Robot, 2015, 31: 850–863
14 He W, Dong Y. Adaptive fuzzy neural network control for a constrained robot using impedance learning. IEEE Trans Neural Netw Learn Syst, 2018, 29: 1174–1186
15 He W, Meng T, He X, et al. Iterative learning control for a flapping wing micro aerial vehicle under distributed disturbances. IEEE Trans Cybern, 2019, 49: 1524–1535
16 Zhao Y R, Song Z B, Ma T Y, et al. A stiffness-adaptive control system for nonlinear stiffness actuators. Sci China Inf Sci, 2019, 62: 050210
17 Liang X Q, Zhao H, Li X F, et al. Force tracking impedance control with unknown environment via an iterative learning algorithm. Sci China Inf Sci, 2019, 62: 050215
18 Li Z, Huang Z, He W, et al. Adaptive impedance control for an upper limb robotic exoskeleton using biological signals. IEEE Trans Ind Electron, 2017, 64: 1664–1674
19 Boaventura T, Buchli J, Semini C, et al. Model-based hydraulic impedance control for dynamic robots. IEEE Trans Robot, 2015, 31: 1324–1336
20 Roveda L, Iannacci N, Vicentini F, et al. Optimal impedance force-tracking control design with impact formulation for interaction tasks. IEEE Robot Autom Lett, 2016, 1: 130–136
21 Yang C, Zeng C, Fang C, et al. A DMPs-based framework for robot learning and generalization of humanlike variable impedance skills. IEEE/ASME Trans Mechatron, 2018, 23: 1193–1203
22 Yang C, Zeng C, Cong Y, et al. A learning framework of adaptive manipulative skills from human to robot. IEEE Trans Ind Inf, 2019, 15: 1153–1161
23 Ajoudani A, Fang C, Tsagarakis N, et al. Reduced-complexity representation of the human arm active endpoint stiffness for supervisory control of remote manipulation. Int J Robot Res, 2018, 37: 155–167
24 Buchli J, Stulp F, Theodorou E, et al. Learning variable impedance control. Int J Robot Res, 2011, 30: 820–833
25 Calinon S, Kormushev P, Caldwell D G. Compliant skills acquisition and multi-optima policy search with EM-based reinforcement learning. Robot Autonom Syst, 2013, 61: 369–379
26 Li Z, Zhao T, Chen F, et al. Reinforcement learning of manipulation and grasping using dynamical movement primitives for a humanoidlike mobile manipulator. IEEE/ASME Trans Mechatron, 2018, 23: 121–131
27 Rozo L, Silvério J, Calinon S, et al. Learning controllers for reactive and proactive behaviors in human-robot collaboration. Front Robot AI, 2016, 3: 30
28 Duan J, Ou Y, Xu S, et al. Learning compliant manipulation tasks from force demonstrations. In: Proceedings of the 2018 IEEE International Conference on Cyborg and Bionic Systems (CBS), 2018. 449–454
29 Ganesh G, Albu-Schäeffer A, Haruno M, et al. Biomimetic motor behavior for simultaneous adaptation of force, impedance and trajectory in interaction tasks. In: Proceedings of the 2010 IEEE International Conference on Robotics and Automation, 2010. 2705–2711
30 Li Y, Ganesh G, Jarrasse N, et al. Force, impedance, and trajectory learning for contact tooling and haptic identification. IEEE Trans Robot, 2018, 34: 1170–1182